# Effect of Particle Shapes on Shear Strength during Direct Shear Testing using GeoPIV Technology

M.I. Peerun[1], D.E.L. Ong[1] and C.S. Choo[1]
[1]Research Centre for Sustainable Technologies, Swinburne University of Technology Sarawak Campus, Malaysia
Email: mpeerun@swinburne.edu.my

**ABSTRACT:** Direct shear tests were performed on reconstituted tunnelling rock spoils to examine the mechanical behaviour of particles during shearing that give rise to cohesion and friction. The tested specimens included sand, along with reconstituted tunnelling rock spoils of metagreywacke obtained from tunnelling sites in Kuching City. Particle interlocking and breakages due to particles angularity were suspected during shearing. Tests on sand exhibited relatively higher values of apparent cohesion due to its strong and rounded particles shape, while metagreywacke exhibited reduced levels of cohesion with high friction due to its weaker matrices of fine angular particles. The levels of apparent cohesion exhibited in the tests were attributed to the shape and angularity of the particles, which influenced the degree of particle interlocking and breakage. In order to assess the particle behaviour during the shearing process, a transparent shear box was purposely fabricated and sequential images were remotely captured using a DSLR camera during the shearing process. GeoPIV, a MATLAB-based script uses Particle Image Velocimetry (PIV) technology to analyse the particle motions through the sequential images captured. The tested specimens showed an increase in cohesion and reduction in friction angles with increasing normal stresses. This is due to greater particle contact area at higher confining pressures, producing greater particles interlocking. The results showed potential linkage between the particle geometry and strength behaviour of the tunnelling rock spoils by using PIV technology. The outcomes of this research would contribute for future assessment of soil arching phenomenon, which can significantly improve the construction design of pipe-jacking works.

**KEYWORDS:** Direct shear, Apparent cohesion, GeoPIV, Interlocking, Particle breakage

## 1. INTRODUCTION

During microtunnelling works through highly fractured rock formations, jacking forces have been found to be geology dependant. A thorough understanding of the highly fractured geology can provide better insight into jacking forces for specific geology, thus leading to economical construction and design. For the highly fractured Tuang Formation in Kuching City, Choo and Ong (2015) successfully back-analysed field measured jacking forces with their original work on characterisation of rock strength parameters by conducting direct shear tests on reconstituted tunnelling rock spoils obtained from the tunnelling sites. From a separate study by Ong and Choo (2015), a redistribution of geostatic stresses occurred due to soil relaxation around the pipe surface. The change in geostatic stresses reduced the soil stresses acting on the pipe crown, allowing the soil to self-stand without collapsing onto the pipe. This phenomenon is known as 'arching'.

To assess the jacking forces measured during pipe-jacking works, Choo and Ong (2015) adopted the jacking force model developed by Pellet-Beaucour and Kastner (2002). The jacking force model takes into account the soil arching phenomenon by incorporating the strength characteristics of the surrounding geology. Choo and Ong (2015) and Ong and Choo (2015) have been conducting direct shear tests on reconstituted tunnelling rock spoils to obtain the equivalent tangential Mohr-Coulomb strength parameters of the highly fracture geology, i.e. tangential internal friction angle, $\varphi'_t$ and tangential apparent cohesion $c'_t$. The developed strength characteristics of the tunnelling rock spoils were used to assess the arching effect with specific geology.

This study focuses on the mechanical behaviour of tunnelling rock spoils of metagreywacke origin compared with sand during different shearing stages. A purpose-built transparent shear box was used to capture sequential images during the shearing process and particle image velocimetry (PIV) technology was used to analyse the particle movements. Vector plots of particle displacement for each of the shearing stages were compared with the stress plots for each tested specimen. Hence, the objective of this study is to assess parameters contributing to apparent cohesion, namely: 1) particle angularity, 2) confining pressure and 3) particle breakage. Better insight on apparent cohesion for specific geology would help to contribute towards future assessment of arching effect.

## 2. TESTED SPECIMENS

The tested specimens were sand and tunnelling rock spoils of metagreywacke origin. The sand consisted of rounded to sub-angular smooth particles, whereas the metagreywacke spoils obtained from the tunnelling sites in Kuching City consisted of angular and rough surfaced particles. Sand can be categorised as orthoquartzite, where extremely strong particles are produced by cementing high content of quartz with silica (Pfeffer 2014). Petrographic analysis of the fined-grained metagreywacke spoils showed that the specimen consisted of poorly sorted angular quartz grains, feldspar grains and rock fragments in a matrix of fine-grained quartz, chlorite, sericite and clay minerals. For fine-grain sediments, the rock strength is relatively weaker due to poor cementation of the grains through binding agents such as calcite, silica or iron oxide (Pfeffer 2014). Figure 1 shows the particle size distribution curves for sand and metagreywacke.

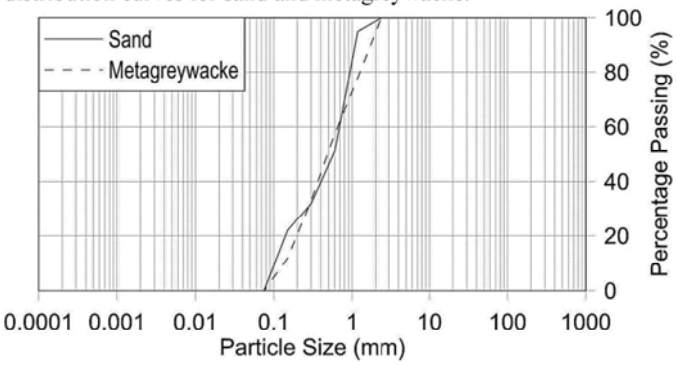


Figure 1 Particle size distribution curve for well-graded sand and poorly graded metagreywacke

The sand specimen was classified as well-graded sand and the metagreywacke specimen as poorly graded tunnelling rock spoils, according to Unified Soil Classification System ASTM (2000).

Table 1 Void ratio before and after shearing of tested specimens

| Specimen | Confining Pressure (kPa) | Volume of Specimen ($m^3$) | Weight of Specimen (kg) | Initial Void Ratio | Change in Void Ratio | Void Ratio after Shearing |
|---|---|---|---|---|---|---|
| Sand | 100 | 0.0000852 | 0.170 | 0.353 | 0.005 | 0.358 |
| | 300 | | | | 0.001 | 0.354 |
| | 500 | | | | -0.002 | 0.351 |
| Metagreywacke | 100 | | 0.160 | 0.438 | 0.005 | 0.443 |
| | 300 | | | | -0.013 | 0.424 |
| | 500 | | | | -0.024 | 0.414 |

Table 1 shows the void ratio before and after the specimens have been sheared at different confining pressures. The void ratio of metagreywacke is greater compared to sand due to its angular particles. The void ratios for both specimens are within the range for coarse sand with no fines as described by Das (2008).

## 3. DIRECT SHEAR TESTING

Direct shear tests were conducted on sand and metagreywacke spoils at varying confining pressures to obtain their strength characteristics. The tests were conducted according to ASTM D 3080 (ASTM 2003). A four-stage shearing model developed by Li and Aydin (2010) was used to understand the particle behaviour during each stages.

### 3.1 Four-stage Shearing Model

According to Li and Aydin (2010), during Stage 1 the sheared sample experiences a change of stress field when subjected to shear force. The particles are rearranged into existing voids within the sample due to the stress field changes. This causes the specimen to contract and the stage is known as 'end zone deformation' (Li and Aydin 2010). Stage 1 ends at the lowest point of initial contraction, where particles interlock with each other to prevent further contraction (Shimizu 1997).

Stage 2 starts from the lowest point of volumetric strain, where particles have to overcome interlocking as the sample densifies due to more contact points among particles. This stage is known as 'particle interlocking', which ends at the attainment of peak shear stress. Peak shear stress is achieved when maximum interlocking has been reached within the shear band. Particle interlocking defines the magnitude that prevents particles from moving from either sliding, rolling or rotating. This makes the sample dilate, corresponding with an increase in volumetric strain.

'Shear zone formation' is the third shearing stage which starts from the peak shear stress and ends when constant residual stress is achieved. The shear band develops into a looser layer due to particle movements (Oda and Kunishi 1974, Fukuoka et al. 2006). The particles rearrange within the shear band, where smaller particles fill into the voids and larger particlesl roll or rotate. This produces a steady shear band structure and causes a reduction in shear resistance.

The last stage known as 'steady shear' is achieved when the sample exhibits no further changes in shear stress or volumetric strain. At this stage, the particles slide at constant amplitude with no significant dilation or compression. The specimen reaches residual state when the specimen exhibits minimal vertical deformation.

## 4. EXPERIMENTAL SETUP

The Geocomp ShearTrac II apparatus was used to conduct direct shear test on the two specimens. To study the particles behaviour during the shearing process, sequential images were to be captured from the test. Hence, a purpose-built transparent shear box was fabricated using Perspex. The transparent shear box was designed according to ASTM D3080 (ASTM 2003) with specimen dimensions of 63.4 mm diameter and thickness 27 mm. Figure 2 (a) and (b) show the test setup and transparent shear box respectively.

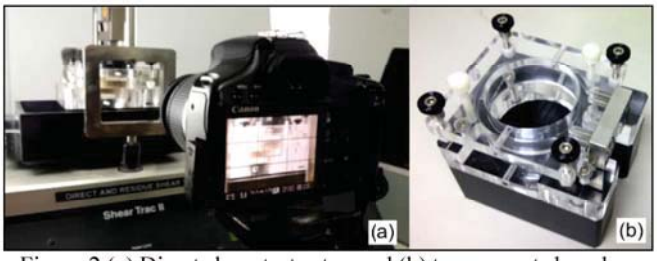


Figure 2 (a) Direct shear test setup and (b) transparent shear box

## 5. GeoPIV

Particle image velocimetry (PIV) technology was developed to study particles flow in fluid mechanics (Adrian 1991). GeoPIV is a MATLAB module, developed by White and Take (2002), which uses the principles of PIV to obtain displacement vectors of particles in geotechnical applications. Sequential images are analysed and input parameters such as patch size, patch spacing, searchzone pixel, frame rate and leapfrog are required to obtain a desirable output result. A Canon EOS450D camera was used to remotely capture sequential images at intervals of 150 s during the direct shear test. A total of 59 images with dimensions of 4272 x 2848 pixels each, were analysed using GeoPIV. A region of interest (ROI) of 30 mm × 5 mm was set along the shear band for all tests, as shown in Figure 3.

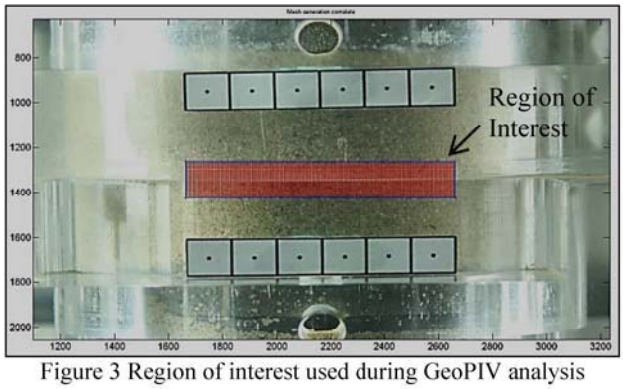


Figure 3 Region of interest used during GeoPIV analysis

## 6. METHODOLOGY

### 6.1 Sample preparation

The tested samples were oven-dried and scalped according to ASTM D 3080 (ASTM 2003), based on the size of the shear box used. The tested particle size distribution was passing 2.36 mm sieve and retained by 75 µm sieve. Choo and Ong (2015) previously adopted the scalping method for direct shear testing of reconstituted tunnelling rock spoils. The specimen was of 63.4 mm diameter and 27 mm thick. The samples were prepared by means of dry pluviation to achieve a dense sample. Sand and metagreywacke were tested at different confining pressures (100 kPa, 300 kPa, and 500 kPa) while being sheared for 15 mm at constant horizontal displacement of 0.0017 mm/s.

### 6.2 GeoPIV analysis

Prior to analysing the particles behaviour during the shearing process, parametric studies were conducted to obtain the most suitable set of parameters to be used for analysing the images captured during direct shear tests. Table 2 shows the input parameters of GeoPIV obtained from the parametric studies.

Table 2 Input parameters for GeoPIV analysis

| Parameter | Inputs |
|---|---|
| Patch size | 16 x 16 pixels |
| Patch spacing | 8 x 8 pixels |
| Searchzone pixel | 8 x 8 pixels |
| Frame rate | 150 seconds |
| Leapfrog | 1 |

## 7. RESULTS

### 7.1 Direct Shear Test Results

Figures 4 (a) and (b) show the shear stress and volumetric plots for sand and metagreywacke spoils, respectively. Sand showed an increase in shear stress from Stage 1 until the end of Stage 2, with a distinct peak shear stress of 383.6 kPa achieved at 500 kPa confining pressure. Shear stress was reduced from Stage 3 to reach residual state during end of Stage 4 producing a residual shear stress of 292.1 kPa at 500 kPa confining pressure. During the initial shearing stage, no compression was found which might be due to the well-graded strong quartz particles found in sand. During Stage 2, the specimen dilated up to 0.1472 mm during confining pressure of 500 kPa. With increasing applied horizontal displacement, the specimen was compressed back to almost its initial thickness at the end of Stage 4.

Metagreywacke spoils showed a similar trend as compared with sand but with a less distinct peak shear stress of 379.3 kPa at 500 kPa confining pressure. With increasing confining pressures, dilation was reduced and hence the metagreywacke specimen was subjected to greater amount of compression. At 500 kPa confining pressure, the sample contracted to a maximum deformation of 0.452 mm. Djipov (2012) stated that angular particles are more subjected to breakages under higher confining pressures. Therefore, it can be noted that metagreywacke specimen contracted more than the sand specimen. In both specimens, the degree of compression was found to be greater with increasing confining pressures. Sand consisting of strong rounded particles experienced greater particle interlocking, hence making the specimen to dilate in comparison to the metagreywacke spoils. Metagreywacke consisting of angular weak matrices of fine grained particles experienced reduced particle interlocking due to particle breakages, hence making the specimen to contract. It can be noted that sand produced higher shear stresses with a distinct peaks as opposed to metagreywacke.

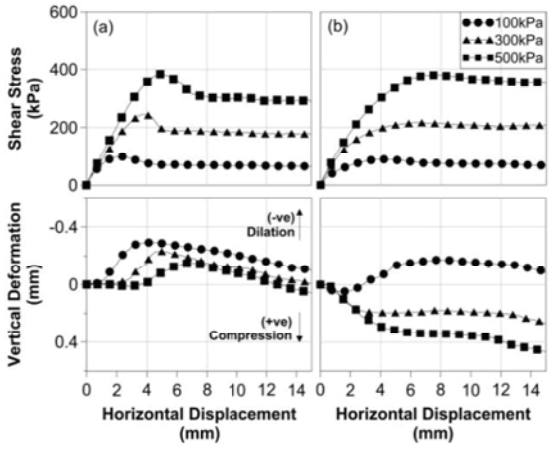


Figure 4 Direct shear results for (a) sand and (b) metagreywacke

Choo and Ong (2015) found that using a conventional best-fit linear Mohr-Coulomb envelope to characterise the strength properties of granular materials over-estimated shear strength at low and high confining pressures. Furthermore, the Mohr-Coulomb failure criterion would under-estimate the shear strength of the sample at intermediate confining pressures. Hence, a non-linear failure criteria was adopted to characterise the strength of the tested specimens. Choo and Ong (2015) successfully adopted a power law method, proposed by De Mello (1977), to obtain non-linear shear strength behaviour materials. A tangential method developed by Yang and Yin (2004) was used to show the degree of nonlinearity in the shear strength of the tested materials. Figures 5 (a) and (b) show the non-linear strength behaviour for sand and metagreywacke respectively. Tangents at 100 kPa and 500 kPa confining pressures were plotted to obtain various tangential friction angle, $\varphi_t'$ and tangential apparent cohesion, $c_t'$ at peak and residual states. Table 3 shows the summary of the nonlinear shear strength results for sand and metagreywacke at peak and residual states, using the tangential method.

From Table 3, it can be concluded that with increasing confining pressures, higher apparent cohesion was achieved. This is due to greater contact area between particles when subjected to higher confining pressures, which resulted in greater particle interlocking. Sand produced higher apparent cohesion as opposed to metagreywacke which is due to the strong quartz particles producing greater particle interlocking occurring during the shearing process. Metagreywacke on the other hand, consisting of weaker matrices of fine-grained particles, were more susceptible to breakages and hence produced less interlocking and lower apparent cohesion. Internal friction angle was found to reduce with increasing confining pressures. Djipov (2012) stated that angular particles subjected to higher interlocking and breakages under high normal stresses would produce a reduction in internal friction angle.

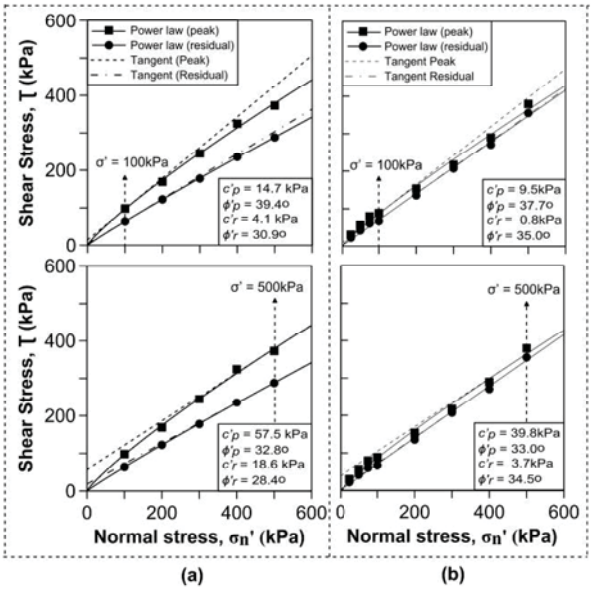


Figure 5 Non-linear strength of (a) sand and (b) metagreywacke at confining pressures of 100 kPa, 300 kPa and 500 kPa

Table 3 Summary of nonlinear shear strength results for sand and metagreywacke at peak and residual states

| Material | Tangent at confining pressure (kPa) | Internal friction angle ($\varphi'$) (°) | | Apparent cohesion ($c'$) (kPa) | |
|---|---|---|---|---|---|
| | | peak | residual | peak | residual |
| Sand | 100 | 39.4 | 30.9 | 14.7 | 4.1 |
| | 500 | 32.8 | 28.4 | 57.5 | 18.6 |
| Metagrey -wacke | 100 | 37.7 | 35.0 | 9.5 | 0.8 |
| | 500 | 33.0 | 34.5 | 39.8 | 3.7 |

### 7.2 GeoPIV Results

During the direct shear tests, sequential images were remotely captured at intervals of 150 seconds until the sample was sheared for 15 mm. GeoPIV software was used to analyse the set of images captured for each test and to produce vector plots of the particles movement during each shearing stage. Figure 6 shows a typical vector plot where the arrows represent the displacement of particles within the tested specimen. The upper half of the shear box remained static during the shearing process, while the bottom half was sheared to the left. Several localised activities were noted from Figure 6, such as: 1) dilation occurring within the upper half of the shear box, 2) particle interlocking along the shear band and 3) localised compression / breakages at the right end-wall of the shear box.

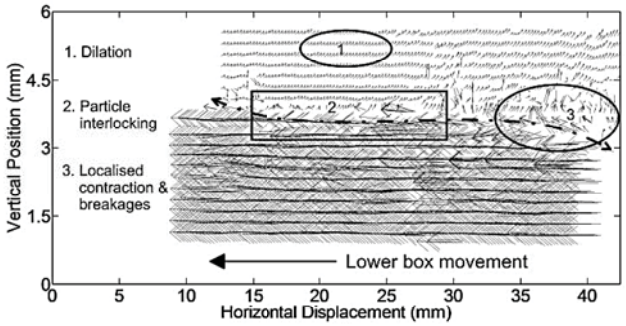


Figure 6 Typical vector plot obtained from GeoPIV showing localized particle activities within the tested specimen

From the vector plots obtained, consistent localised activities were captured within the test specimens. In Figure 6, the dashed line illustrates a pattern showing particles on the right end of the shear box moving downwards and particles on the left end of the shear box moving upwards. Several researchers observed such micromechanical behaviour while studying the shear band through discrete element modelling (O'Sullivan et al. 2006, Kang et al. 2012, Indraratna et al. 2014, Salazar et al. 2015).

To provide better understanding of particle movements during each of the shearing stages, a combination of direct shear test results and GeoPIV results at confining pressure of 500 kPa are shown in Figures 7 and 8 for sand and metagreywacke, respectively. From Figure 7, during the first stage of shearing for sand specimen, the volumetric plot shows no change in vertical displacement. The vector plot during Stage 1 confirms this observation, where the particles moved horizontally to the left with no vertical movement. Peak shear stress was achieved by end of Stage 2 with the volumetric plot showing dilation of the specimen. Stage 2 vector plot shows localised interlocking and particles moving upwards representing dilation. During Stage 3, the shear stress decreased corresponding with a reduction in dilation from the volumetric plot. This was due to a reduction in interlocking and dilation activities as shown in Stage 3 vector plot. Stage 4 produced a constant residual shear stress while the sample was compressed to almost zero vertical displacement. Stage 4 vector plot shows localised compression at the right end of the shear box and no vertical movement at the other end of the shear box. Such localised activities at the right end of the shear box was also found in Figure 8 and previously stated by Shimizu (1997) which is due to localized strains at the end zones of the shear band.

From Figure 8, compression was observed from the volumetric plot during Stage 1. The vector plot during Stage 1 confirms this observation, where particles moved downwards due to localized compression. The volumetric plot at Stage 2 showed reduced compression of the specimen which can be portrayed in the vector plot, where minimal dilation with particles moving upwards prevented the specimen to further compress. A less distinct peak shear stress was achieved by end of Stage 2 due to lesser interlocking activities as opposed to sand specimen. During Stage 3, the volumetric plot showed minimal vertical displacement.

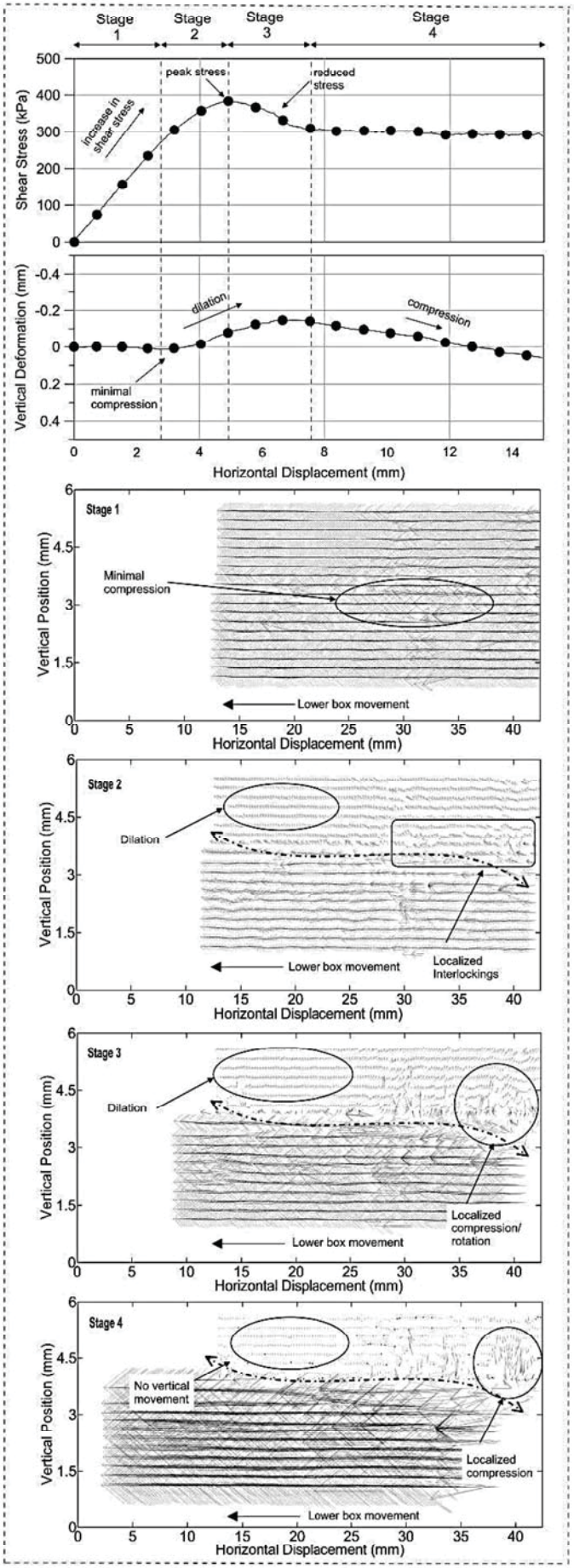


Figure 7 Direct shear test results and vector plots for each shearing stage of sand at confining pressure of 500 kPa

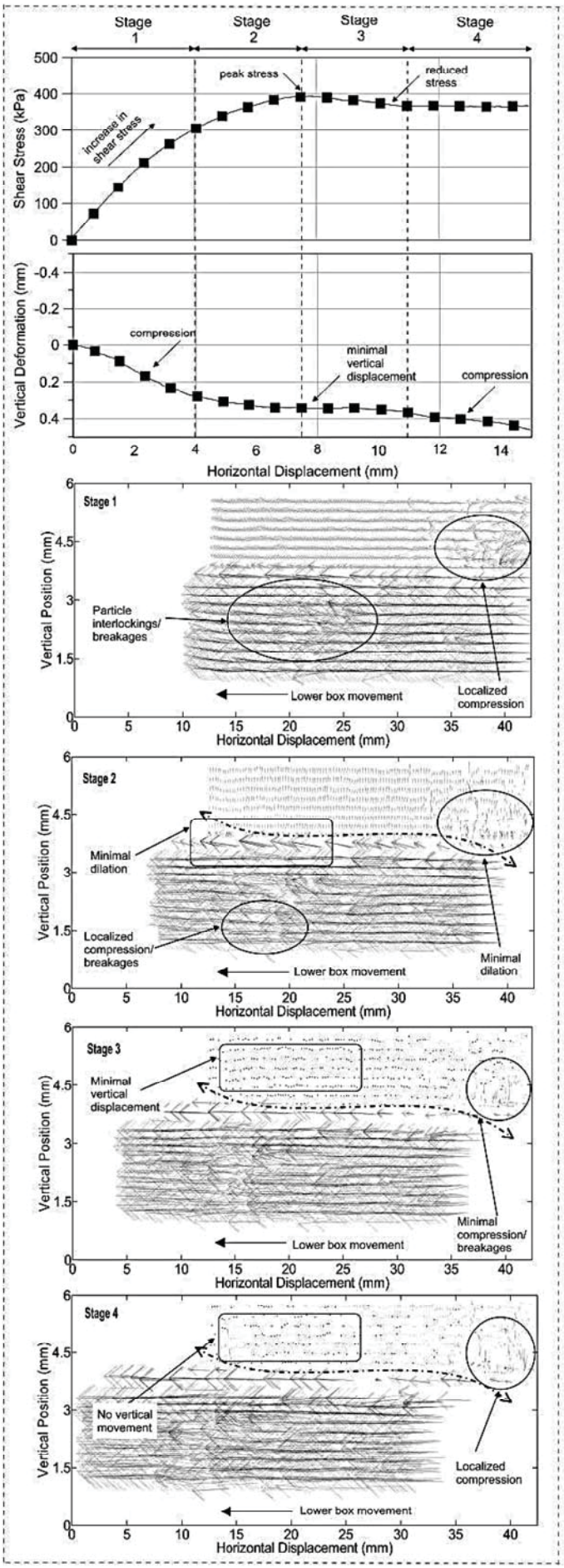


Figure 8 Direct shear test results and vector plots for each shearing stage of metagreywacke at confining pressure of 500 kPa

The vector plot showed similar behaviour where minimal compression and no dilation were recorded. During the last stage, the specimen was further compressed which was also shown in the vector plot at Stage 4 due to localized compression. Throughout all the shearing stages, the volumetric plot shows continuous compression at a maximum deformation of 0.438mm. The vector plots in Figure 8 consistently show localised compression within the specimen resulting into a reduced shear stress as compared to the sand specimen.

## 8. DISCUSSION

### 8.1 Effect of particle shape on particle interlocking and breakages

Particle angularity is one of the factors affecting the shear strength of the test specimen. Particle breakages are expected mostly in angular particles as the stresses are concentrated at the edges and consist of more voids within the sample as opposed to rounded ones (Djipov 2012). The well-graded sand specimen consisted of rounded to sub-angular quartz particles with smooth surface whereas the tunnelling rock spoils of metagreywacke origin contained angular particles of weak matrix of fine-grained quartz, sericite, chlorite and clay minerals. The rounded particles of sand produced lower void ratio as opposed to the angular particles of metagreywacke. Hence, greater contact forces among the quartz particles in the sand specimen resulted in greater interlocking, causing the sand sample to dilate. In contrast, greater voids within the weaker matrices of metagreywacke created less points of contact between the metagreywacke spoils.

This, combined with the highly angular metagreywacke spoils, created stress concentrations and produced particle breakages. Smaller particles resulting from these breakages would fill the existing voids and result in compression of the metagreywacke specimen. Figures 4 (a) and (b) showed that at confining pressure of 500 kPa, the sand specimen dilated to a maximum vertical displacement of 0.147 mm whereas metagreywacke specimen was compressed to a maximum of 0.452 mm. Figures 7 and 8 confirm these observations of particle activities between sand and metagreywacke, respectively. During Stages 2 and 3, the vector plots showed that the sand specimen exhibited a significant dilation throughout the sample, whereas the metagreywacke spoils demonstrated minimal dilation together with localised compression / breakages.

### 8.2 Effect of particle interlocking and breakages on apparent cohesion

Particle interlocking is applicable for all types of soils, inclusive of clay and gravel. Particle interlocking produces the peak shear strength which results in apparent cohesion (Taylor 1948, Schofield 1998). Sand consisting of lesser voids produced more points of contact between the particles resulting in greater interlocking within the strong quartz particles. This resulted in the dilation of the sand specimen, which can be seen at Stages 2 and 3 of Figure 7. For the metagreywacke specimen, larger void ratio within the sample resulted in localised compression due to particle breakage. These breakages were observed in Stages 2 and 3 of Figure 8.

From Figure 4 (a), sand produced a distinct peak shear stress of 383.6 kPa, corresponding with a dilation of 0.147 mm due to particle interlocking. Metagreywacke produced a reduced peak shear stress of 379.3 kPa with a compression of 0.452 mm due to particle breakages, as shown in Figures 4 (b) and 8. The effects of particle interlocking and particle breakages can have significant effects on the shear strengths of the specimens. From Table 2, metagreywacke produced lower apparent cohesion at 100 kPa and 500 kPa confining pressures due to particle breakages, as opposed to sand which exhibited greater amount of apparent cohesion due to the effect of particle interlocking.

### 8.3 Effect of confining pressure on apparent cohesion

At higher normal stresses, the tested specimen compresses and greater interlocking among particles produces higher shear strength of the sample (Xiao et al. 2014). Both specimens produced higher apparent cohesion at peak and residual states with increasing confining pressure (Table 3). Also, the soil internal friction angle decreases with increasing confining pressure. Sand particles exhibiting higher amount of interlocking activities, consistently produced higher apparent cohesion than metagreywacke. Figures 9 (a) and (b) show the vector plots of metagreywacke during Stage 3 at confining pressures of 100 kPa and 500 kPa respectively. At 100 kPa (Figure 9 (a)), the sample dilates due to interlocking whereas at 500 kPa (Figure 9 (b)), the sample compresses due to higher confining pressure. Hence, this confirms that higher confining pressure will compress the sample producing greater contact area among particles.

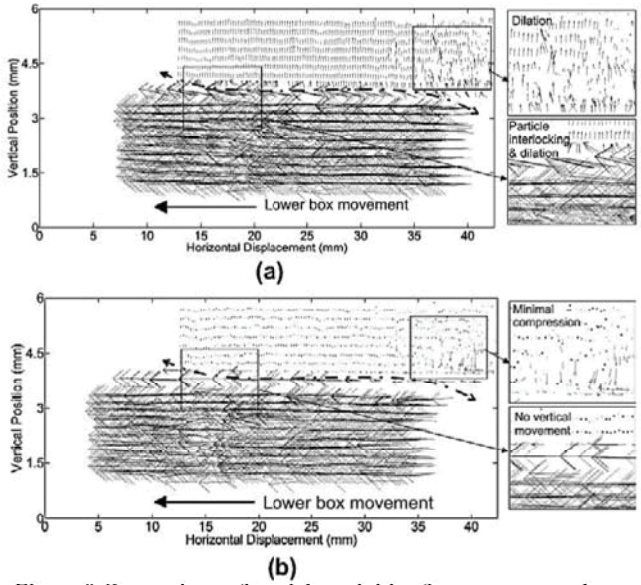


Figure 9 Comparison of particle activities for metagreywacke at confining pressures of (a) 100 kPa and (b) 500 kPa during shearing Stage 3

## 9. CONCLUSION

The study of mechanical behaviour of sand and tunnelling rock spoils of metagreywacke origin was conducted during direct shear testing using particle image velocimetry technology. Particle angularity was one of the factors affecting the strength properties of the tested samples. Sand consisted of strong rounded quartz particles whereas metagreywacke consisted of angular particles. Metagreywacke particles consisted of weak matrices of fine-grained materials bonded together. This study focused on the factors contributing towards the apparent cohesion of the tested materials, which was found to be important for the assessment of soil arching. A power law was adopted to obtain the strength properties of the non-linear behaviour materials. Direct shear test and GeoPIV results were combined and analysed together to produce the following observations: 1) Angular particles with high void ratio are more susceptible to breakages are opposed to rounded ones; 2) Particle with high quartz content will produce more interlocking; 3) Particle breakages will reduce the shear strength of the sample; 4) Increasing confining pressures will produce a reduction in internal friction angle and an increase in cohesion. This study has successfully shown the mechanical behaviour of particles with relation to its strength characteristics, which would be a useful contribution in future assessment of soil arching during pipe-jacking works.

## 10. ACKNOWLEDGEMENT

The authors would like to extend their appreciation to Hock Seng Lee Bhd, Jurutera Jasa (Sarawak) Sdn Bhd as well as David White.

## 11. REFERENCES

Adrian, R. J. (1991). "Particle imaging techniques for experimental fluid mechanics." J. Fluid. Mech. 23: 261-304.

ASTM (2000). Standard practice for classification of soils for engineering purposes (unified soil classification system). D2487-00, West Conshohocken, PA.

ASTM (2003). Standard test method for direct shear test of soils under consolidated drained conditions. D3080-03, West Conshohocken, PA.

Choo, C. S. and D. E. L. Ong (2015). "Evaluation of Pipe-Jacking Forces Based on Direct Shear Testing of Reconstituted Tunneling Rock Spoils." Geotech. Geol. Eng.

Das, B. M. (2008). "Advanced soil mechanics." Third Edition, Taylor & Francis, London and New York.

De Mello, V. F. B. (1977). "Reflections on design decisions of practical significance to embankment dams." Geotechnique 27(3): 281-354.

Djipov, D. N. (2012). Effectes of particle breakage on the compression and shear behavior of carbonate sand. 1st Civil and Env. Eng. Student Conference, Imperial College London.

Fukuoka, H., et al. (2006). "Observation of shear zone development in ring-shear apparatus with a transparent shear box." Landslides, Springer-Verlag 3(3): 239-251.

Indraratna, B., et al. (2014). "Behavior of Fresh and Fouled Railway Ballast Subjected to Direct Shear Testing: Discrete Element Simulation." Int. J. Geomech. 14(1): 34-44.

Kang, D. H., et al. (2012). Pore Directivity of Soils Subjected to Shearing: Numerical Simulation and Image Processing. GeoCongress 2012: 2342-2351.

Li, Y. R. and A. Aydin (2010). "Behavior of rounded granular materials in direct shear: Mechanisms and quantification of fluctuations." Eng. Geology(115): 96-104.

O'Sullivan, C., et al. (2006). Experimental Validation of Particle-Based Discrete Element Methods. GeoCongress 1-18.

Oda, M. and J. Kunishi (1974). "Microscopic deformation mechanism of granular material in simple shear." Japan Society of Soil Mech Foundation 14(4): 25-38.

Ong, D. E. L. and C. S. Choo (2015). "Back-analysis and finite element modeling of jacking forces in weathered rocks." Tunnelling Underground Space Technol.(51): 1-10.

Pellet-Beaucour, A. L. and R. Kastner (2002). "Experimental and analytical study of friction forces during microtunneling operations." Tunneling Underground Space Technol. 17(1): 83-97.

Pfeffer, W. T. (2014) Sedimentary Rocks, CVN 3698 Engineering Geology Spring. INSTAAR Dept. Civil. Env. Architectural Eng,University of Colorado

Salazar, S. E., et al. (2015). "Development of an Internal Camera–Based Volume Determination System for Triaxial Testing." Geotechnical Testing Journal 38(No. 4,): 549–555.

Schofield, A. N. (1998). The Mohr-Coulomb Error, 3.2 Critical states and apparent cohesion, Eng. Department, Division D Soil Mechanics Group, Cambridge University.

Shimizu, M. (1997). "Strain fields in direct shear box tests on a metal-rods model of granular soils. In: Asaoka, Adachi, Oka." Deformation and Progressive Failure in Geomechanics: 151-156.

Taylor, D. W. (1948) Fundamentals of soil mechanics. John Wiley and Sons, New York

White, D. J. and W. A. Take (2002). GeoPIV: Particle Image Velocimetry (PIV) software for use in geotechnical testing. Technical report, , Eng. Dept. Cambridge University

Xiao, Y., et al. (2014). "Strength and Deformation of Rockfill Material Based on Large-Scale Triaxial Compression Tests. I: Influences of Density and Pressure." Journal of Geotechnical and Geoenvironmental Engineering 140(12): 04014070.

Yang, X. L. and J. H. Yin (2004). "Slope stability analysis with nonlinear failure criterion." J. Eng. Mech. 130(3): 267-273.